

Zinc sorption by permanganate treated pine chips



R.G. McLaughlan^{a,*}, S.M.G. Hossain^a, Othman A. Al-Mashaqbeh^b

^a Faculty of Engineering and Information Technology, University of Technology Sydney (UTS), P.O. Box 123, Sydney, NSW 2007, Australia

^b Scientific Research Centre, Royal Scientific Society, Amman 11941, Jordan

ARTICLE INFO

Article history:

Received 9 March 2015

Accepted 23 May 2015

Available online 30 May 2015

Keywords:

Consumption

Kinetics

Oxidation

Permanganate

Pine chips

Sorption

ABSTRACT

The sorption equilibria and kinetics of zinc from aqueous solution on both untreated and permanganate treated pine chips were investigated. The sorption kinetics were best described by pseudo-second-order equation and the sorption isotherms were well fitted by a Langmuir model for both untreated and treated pine chips. Zinc sorption increased from 1.2 mg g^{-1} in untreated samples to 3.9 mg g^{-1} for the treated pine chips. Analysis shows that the carboxylic content increased after oxidative treatment of wood sorbents. This was responsible for the improved sorption of zinc onto the pine chips. The permanganate-wood reaction rate in batch experiments was biphasic first-order with an initial rate (0–25 min) and then a slower rate (25–807 min). The initial rates were approximately 3 times greater than the later stage rates. The reaction rates was also particle size dependent with the rate for 4.75 mm pine chips, 11–19% less than that of the 1.18 mm pine chips. Rate limiting mechanisms included intra-particle mechanism of MnO_4^- interaction with pine chips is complex and consisting of surface external mass transfer as well as intra-particle diffusion. Rate-limiting reactions in the column caused the shape of the breakthrough curve to exhibit tailing.

© 2015 Elsevier Ltd. All rights reserved.

Introduction

Zinc and other heavy metals can be introduced into the water environment from metal plating, mining operations, alloy processing and sewage sludge. Dissolved zinc can have a significant adverse impact on the environment and human health [1,2]. Various methods such as reverse osmosis, ion exchange, coagulation and sorption can be applied for the removal of dissolved metals from aqueous solution. Among these methods, sorption is the most widely used and is effective when well-designed [3,4]. Wood has potential as a sorbent due to its physico-chemical characteristics, low-cost and widespread availability. Wood contains lignin, cellulose and hemicellulose which can be utilized to sorb a variety of organic compounds [5,6] and heavy metals [7]. In recent years, agricultural by-products (e.g. wood, pine bark, sawdust, compost and leaves) have been widely used as bio-sorbents for metal removal [8,9]. The direct use of these bio-sorbents is often limited due to their low sorption capacity. Therefore, cost-effective chemical treatments are needed to improve the sorbent capacity of wood materials.

Woody biomass can be treated with permanganate to enhance the sorption capacity. Studies found that the oxidation of lignocellulosic material with permanganate had a rapid initial reaction as well as increasing the carboxylic group content [10,11]. Jolly et al. [12] oxidized a lignocellulosic substrate by permanganate at pH~2 and improved the binding capacity of the material for Cu by 32% and Zn by 41%. Infrared (IR) results indicated that oxidation of the lignin created carboxylic (COOH) groups. While the impact of permanganate treatment on sorption has been studied using different types of woody biomass, there is little work on the reaction kinetics between wood and permanganate. This knowledge is needed for the design and optimization of permanganate treatment of wood.

The aim of this study is to evaluate the capacity and performance of permanganate treated pine chips in the removal of zinc from aqueous solution as well as to examine the reactivity and kinetics between wood chips (pine) and permanganate. The reactivity between wood and permanganate were further investigated under dynamic conditions using column studies. The Attenuated Total Reflection Fourier Transform Infrared Spectroscopy (ATR-FTIR) was used to investigate the surface functionalization of untreated and treated pine chips. It is expected such information will give insight into aqueous metal removal by modified pine chips and provide the basis for further development

* Corresponding author. Tel.: +61 295142614.

E-mail address: robert.mclaughlan@uts.edu.au (R.G. McLaughlan).

of modified wood sorbents engineered for improved sorption using complex wastewaters.

Experimental methodology

Pine chip material preparation and characterization

The pine chips (Superior Pine Chip) were supplied by Soilco Pty Ltd., Australia. The pine chips were sieved such that 4.75 mm material passed through a 6.5 mm sieve but was retained over a 4.75 mm mesh sieve and 1.18 mm passed through a 2.36 mm mesh sieve but was retained over a 1.18 mm mesh sieve. Visible contamination from pine bark fragments were removed prior to processing. All samples were washed with distilled water and dried in an oven at 50 °C for 48 h, then stored in an airtight desiccator at room temperature (22 °C) until use. All weights reported in the paper are as dry matter.

Lignin, cellulose, and hemicellulose contents were determined using methods for Acid Detergent Fibre, Acid Detergent Lignin-Neutral Detergent Fibre [13]. Total carbon and nitrogen content for all solid materials were determined in duplicate using a TRU-SPEC carbon nitrogen determinator. The cation exchange capacity (CEC) of the pine chips was measured using saturated ammonium extractants at pH 7 [14]. The specific surface areas and pore characteristics of solid phase media were measured using Brunauer–Emmett–Teller (BET/N₂) (Micromeritics Tristar). Measured pine chips surface area and pore volume data (Table 1) are similar to other reported values for wood [15,16] and the CEC is consistent for pine [17]. The variability between the size fractions in-terms of C/N ratio, particle size and pore width is likely due to sample variability and may represent some bark attached to the pine chips. It should be noted that the particles are highly elongate as a result of the grinding and sieving process [18].

Batch oxidation experiment

About 5 g of untreated pine chips were reacted at pH~2 in a 300 mL amber colour glass bottle with 250 mL of ~61 mM MnO₄⁻ and mixed in an orbital shaker at 150 rpm at 22 °C. An aliquot (~0.15 mL) of liquid samples were withdrawn at preselected time intervals and analysed for residual permanganate. All experiments were carried out in duplicate. The maximum deviation at absorbance 525 nm from the mean on any sample was less than 2%.

Column oxidative experiment

The columns were constructed in PVC pipe class 18 and sealing by a PVC cap at the end of the column using Silastic. All columns were packed by mixing 66 g of pine chips (4.75 mm) and 1665 g of 0.6 mm glass beads (~20–25% v v⁻¹ pine) with a bed depth of approximately 54 cm long by 5.3 cm internal diameter (I.D.) and bulk density 1.5 g cm⁻³. Both ends of the column were packed by a

layer of 1.5 cm of glass bead (3 mm) to ensure uniform flow. These glass beads (3 mm) are separated by plastic mesh at either ends. The inlet solutions were pumped from a 25 L plastic container at a constant flow rate and at a constant hydraulic head using peristaltic pump (Masterflex Model 7553-85) into the column under up flow directions. The control column was packed with glass bead and showed no evidence for the consumption of KMnO₄ due to contact with the column apparatus. Before start-up, the column was operated for approximately 12–24 h by passing distilled water until a steady flow, as well as stable conductivity and colour occurred.

A chloride tracer test was carried out to determine the column pore volume. This was undertaken both before the MnO₄⁻ injection and after MnO₄⁻ injection. The column was initially flushed with distilled water at flow rate ~5 mL min⁻¹ for 24 h. The tracer solution (KCl, ~72 mg L⁻¹) was prepared and pumped through the column at a flow rate of ~5 mL min⁻¹. This test was used to determine the pore volume of the column and to compare the tracer and permanganate breakthrough curves. The effective porosity for the column filtration media was calculated from the total internal column volume (1232 mL) and the pore volume with relative concentration (C/C₀) at 0.5 which is one pore volume. Therefore, one pore volume in the column is equal to 525 and 517 mL for pre and post MnO₄⁻ injection tracer, with a corresponding porosity 0.43 and 0.42, respectively, at flow rate 5 mL min⁻¹. Thus the effective pore volume as determined by the tracer test is used in normalizing the accumulated effective volume of permanganate breakthrough curves. The tracer test was then followed by distilled water flush. All experiments were carried out at 22 °C.

The permanganate treatment of the pine chips was undertaken in-situ by injecting an aqueous solution (pH~2) of KMnO₄ ~61 mM at a flow rate ~5 mL min⁻¹ into the column after the distilled water flushing. During oxidant injection, effluent samples (20 mL) were collected from the outlet of the column at various times for MnO₄⁻ analysis. Injection was continued until the concentration of KMnO₄ measured in the effluent changed less than 2% of the previous reading. This indicated steady state. Then the columns were drained and flushed with distilled water until MnO₄⁻ was no longer detected in the effluent. The breakthrough curve for oxidation of KMnO₄ onto the pine chips was obtained by plotting C (effluent concentration) divided by C₀ (inlet concentration) against number of column pore volumes. The effective column pore volume was determined by a chloride tracer test. The total quantity of permanganate consumed in the column was calculated from the area above the breakthrough curve (outlet KMnO₄ concentration, C/C₀ versus time) multiplied by the flow rate. The consumption capacity of the pine chips were calculated from the mass consumed in the column divided by the mass of the pine chips (66 g) in the column.

Batch zinc sorption experiment

Batch sorption studies were conducted by placing 100 mL of a known concentration of zinc solution with a known weight of untreated and treated pine chips (1.18 mm size) in separate 250 mL Erlenmeyer flasks. For the batch kinetic tests these flasks were then shaken at 150 rpm for a specified time period and then analysed for residual concentration of Zn(II). Batch equilibrium sorption experiments were carried out by contacting ~0.2 g of pine chips with different initial concentrations of zinc aqueous solution (1–40 mg L⁻¹) at pH (~5) in separate flasks. The flasks were shaken for 72 h at room temperature (22 °C). All experiments of Zn(II) sorption were carried out in triplicate and the maximum deviation of residual concentration of zinc from the mean was less than 3%. Before analysis, all samples from each flask were decanted and filtered through a 0.2 μm Whatman filter paper.

Table 1
Physico-chemical properties of pine.

Parameters	Pine chips	
Particle size (mm)	1.18	4.75
BET surface area (m ² g ⁻¹)	0.45	0.79
Pore width (nm)	10.0	15.6
Total carbon (mg g ⁻¹)	98.9	95.6
CEC (cmol kg ⁻¹)	6.2	6.2
Nitrogen (mg g ⁻¹)	0.23	0.16
Lignin (%)	23	23
Cellulose (%)	57	57
Hemicellulose (%)	14	14

The permanganate treated pine chips used in the batch zinc sorption tests were prepared by reacting untreated pine chips at pH~2 in a 300 mL amber colour glass bottle with 250 mL of ~61 mM MnO_4^- . This was mixed in an orbital shaker at 150 rpm and 22 °C for 24 h. The treated pine chips were then filtered using a fine sieve, washed several times with Milli-Q water until the pH remained neutral, then dried in an oven at 50 °C for 48 h.

Sorption data analysis

The amount of zinc sorbed, q_t (mg g^{-1}), onto the solid phase at time t , was calculated according to Eq. (1):

$$q_t = \frac{V(C_o - C_t)}{W} \quad (1)$$

where C_o is the initial metal concentration (mg L^{-1}), C_t is the residual metal concentration in the liquid phase (mg L^{-1}) at time t ; V is the volume of the solution (L) and W is the mass of the sorbent (g).

Equilibrium sorption capacity, q_e (mg g^{-1}), was calculated by Eq. (2):

$$q_e = \frac{V(C_o - C_e)}{W} \quad (2)$$

where C_e (mg L^{-1}) is the equilibrium metal concentration in the liquid phase after treatment for a certain period of time.

The kinetic data were modelled using both the pseudo-first-order and pseudo-second-order equations. The pseudo-first-order equation is expressed by Eq. (3):

$$q_t = q_e(1 - e^{-k_1 t}) \quad (3)$$

where q_e and q_t are the sorption capacities (mg g^{-1}) at equilibrium and time t , respectively, and k_1 is the rate constant of pseudo-first-order sorption (h^{-1}).

The pseudo-second-order equation is expressed by Eq. (4):

$$\frac{1}{(q_e - q_t)} = \frac{1}{q_e} + k_2 t \quad (4)$$

where q_e and q_t are the sorption capacities (mg g^{-1}) at equilibrium and time t , respectively, and k_2 is the rate constant of pseudo-second-order sorption ($\text{g mg}^{-1} \text{h}^{-1}$).

Sorption isotherm data were described by the two most widely used models. The Langmuir model is expressed by Eq. (5):

$$q_e = \frac{Q \times b \times C_e}{(1 + bC_e)} \quad (5)$$

Freundlich model is expressed by Eq. (6):

$$q_e = KC_e^n \quad (6)$$

where C_e is the equilibrium concentration in the liquid phase (mg L^{-1}) and q_e is the equilibrium sorption capacity of the sorbent (mg g^{-1}). Parameter Q represents the maximum sorption capacity (mg g^{-1}) with monolayer coverage on the sorbent particle while b is the Langmuir constant related to the free energy of sorption (L mg^{-1}). K is the sorption capacity constant, n is the Freundlich constant for surface heterogeneity.

Sorption isotherm models were fitted against experimental data using nonlinear regression within a Microsoft Excel spreadsheet [19]. This approach was used rather than linearization of the equations since linearization may result in improperly weighted data points during the analysis [20] and limit the accuracy of the fit [19]. The mathematical models were optimized for best fit using sum of error squares (SSE). Parameter fits with the lowest SSE values were considered best-fit. Regression coefficients (r^2) were also calculated. The (SSE) was calculated by Eq. (7):

$$SSE = \sqrt{\frac{\sum (q_{e,\text{exp}} - q_{e,\text{calc}})^2}{N}} \quad (7)$$

where, $q_{e,\text{exp}}$ and $q_{e,\text{calc}}$ are the sorption capacity (mg g^{-1}) obtained from experiment and calculation, respectively, and N is the number of data points.

The intra-particle diffusion rate can be expressed by Eq. (8):

$$q_t = k_{\text{id}} t^{0.5} + c \quad (8)$$

where k_{id} is the intra-particle diffusion rate constant, q_t is the amount sorbed per unit sorbent at time t and c is a constant.

Analytical methods

The residual concentrations of permanganate were analysed with a UV-visible spectrophotometer (Shimadzu, Model UV-1700, Japan). Further details of the analysis method are elsewhere [21]. Stock solution of zinc (1000 mg L^{-1}) was prepared by using $\text{Zn}(\text{NO}_3)_2 \cdot 6\text{H}_2\text{O}$ (zinc hexahydrate nitrate) in Milli-Q water. Different working concentrations of zinc were prepared by diluting the stock solution. The pH of the zinc solution was adjusted (~5) using dilute nitric acid (HNO_3) and sodium hydroxide (NaOH) solutions. All chemical reagents used in this study were of analytical grade. $\text{Zn}(\text{II})$ samples from the batch (10 mL) tests were filtered and preserved by acidifying to $\text{pH} < 2$ using dilute HNO_3 [22] prior to analysis. The residual zinc concentration was analysed using Agilent 4100 MP-AES Spectrometer (Microwave Plasma-Atomic Emission Spectrometry). Chloride samples were analysed by ion chromatography (Dionex DX-600). ATR-FTIR method was used for analysis of the surface of KMnO_4 treated and untreated pine chips. ATR-FTIR scans were collected in the range $4000\text{--}800 \text{ cm}^{-1}$ and 4 cm^{-1} resolution.

Results and discussion

Batch oxidative studies

The consumption of KMnO_4 as MnO_4^- by pine chips after 807 min of reaction time were 436 and 453 mg g^{-1} for the particle size ranges 4.75 and 1.18 mm, respectively (Fig. 1).

In the reaction time 0–807 min for both particle size ranges, the lower r^2 and higher SSE value for zero-order and second-order suggests that the first-order kinetic model was best fit to the observed data (Table 2).

The consumption of permanganate can be better modelled as a first-order rate using a two-step process for both particle sizes (Fig. 2a,b and Table 3).

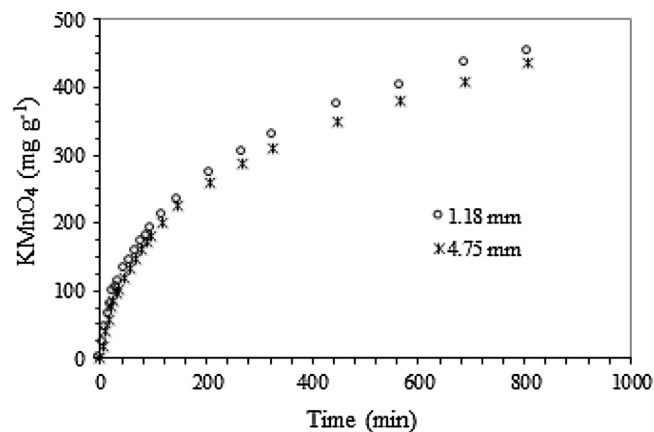
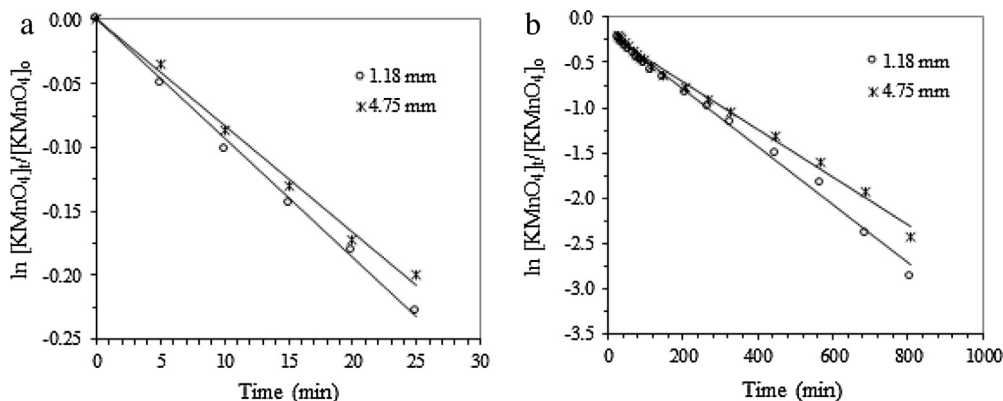


Fig. 1. Kinetic plots for KMnO_4 by reaction with pine.

Table 2The kinetic parameters for 0–807 min reaction of KMnO_4 with pine.

Pine (mm)	Zero-order			First-order			Second-order		
	k (mM min^{-1})	r^2	SSE	k_1 (min^{-1})	r^2	SSE	k_2 ($\text{mM}^{-1} \text{min}^{-1}$)	r^2	SSE
1.18	0.0949	0.501	11.7	0.0036	0.973	5.0	0.0002	0.822	6.0
4.75	0.0897	0.530	10.8	0.0030	0.956	5.4	0.0002	0.878	6.8

 k , zero-order rate constant; k_1 , first-order rate constant; k_2 , second-order rate constant.**Fig. 2.** Kinetic fit curves of pine and KMnO_4 : (a) reaction time 0–25 min, (b) reaction time 25–807 min.**Table 3**The first-order kinetic parameters for the reaction of KMnO_4 with pine.

Pine (mm)	0–25 min			25–807 min		
	k_1 (min^{-1})	r^2	SSE	k_1 (min^{-1})	r^2	SSE
1.18	0.0093	0.996	0.26	0.0032	0.995	6.4
4.75	0.0083	0.994	0.30	0.0026	0.993	7.0

 k_1 , first-order rate constant.

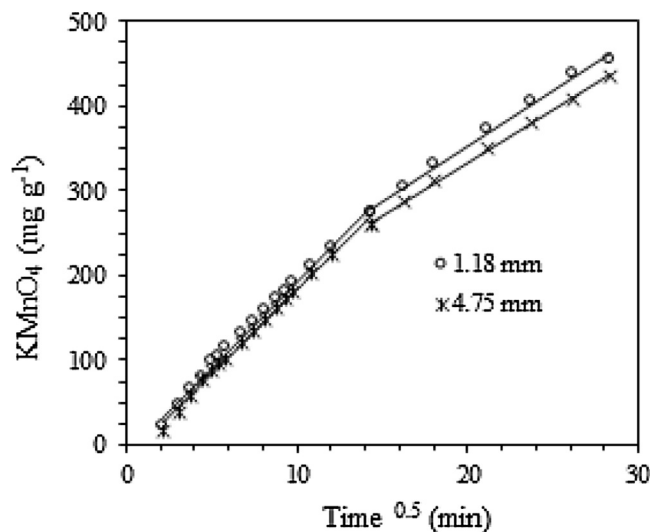
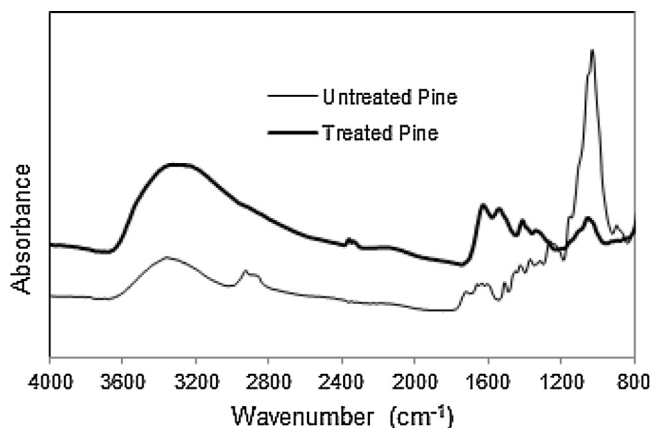
This biphasic reaction rate is consistent with permanganate reaction with lignin [23]. Tong et al. [23] found that the reaction rate is more rapid in the initial stage (within 30 min) and suggested that the rapid reaction of KMnO_4 may preferentially utilize the easily oxidizable parts of lignin present in wood. The reaction of permanganate with cellulose was also found to be biphasic [11] with an initial rate of 0.0021 min^{-1} .

An intra-particle diffusion model was applied to the permanganate reaction rate data to better understand the rate controlling mechanisms. Numerous studies on intra-particle diffusion model show that initial curved portions of the intra-particle diffusion plot suggest film diffusion processes while linear portions suggest intra-particle diffusion [24]. A third stage may occur where intra-particle diffusion decreases due to a low solute concentration. However the rate controlling mechanism may change during the sorption process.

The mechanisms responsible for the observed change in the permanganate reaction rate with this study cannot be determined. It could in part be due to heterogeneous reactions sites on the wood surface or it could be due to intra-particle diffusion during transport of the permanganate within the particle. The intra-particle diffusion plots shows two linear trends (Fig. 3).

The 4.75 mm particle has a slightly lower uptake rate than the 1.18 mm particle size. This slight difference is consistent with previous work showing relatively little change in wood particle diameter with increased sieve mesh size [18].

To gain insight into the physico-chemical changes in pine due to permanganate oxidation, ATR-FTIR scans were used (Fig. 4).

**Fig. 3.** Intra-particle diffusion plot of KMnO_4 interaction with pine.**Fig. 4.** ATR-FTIR spectra of untreated and treated pine.

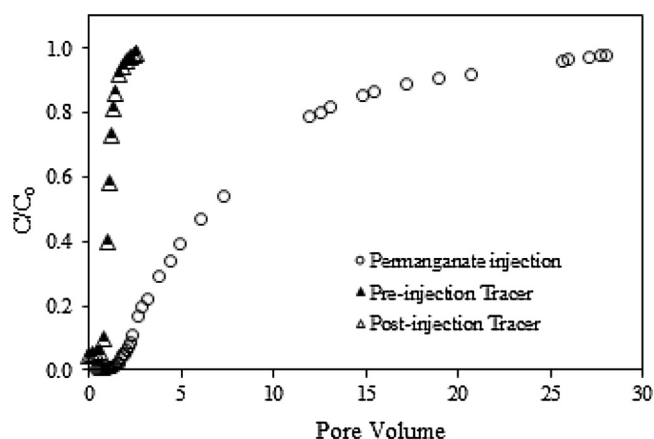


Fig. 5. Column breakthrough curves.

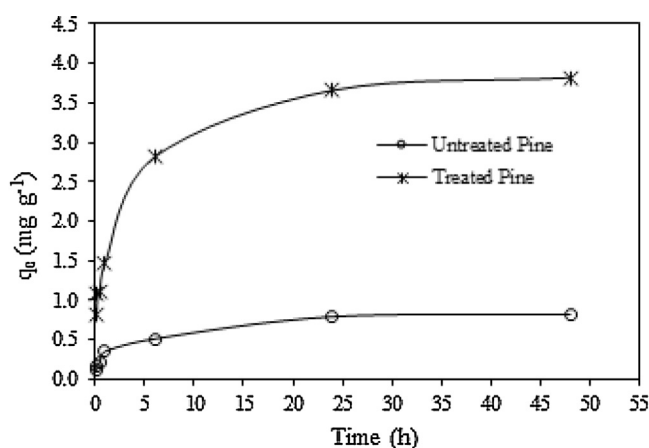


Fig. 6. Sorption kinetics of Zn(II) onto pine.

A strong hydrogen bonded O–H stretching vibration was found around 3406 cm^{-1} which was attributed to water molecules sorbed in the wood [25]. The peak at 3406 cm^{-1} was shifted to 3390 cm^{-1} and broadened ($3259\text{--}3390\text{ cm}^{-1}$) and intensified after permanganate oxidation. This peak is attributed to the O–H stretching vibration in the carboxylic acid group [26].

Kostic et al. [27] found that the chemical structure of cellulose is changed upon oxidation of hydroxyl group into the corresponding carboxyl structure. The peak of alcohol (OH group) at 1033 cm^{-1} [28] was decreased after oxidation and the OH in cellulose structure is oxidized into COOH [29]. The decrease of absorption at 1033 cm^{-1} could be due to permanganate oxidation of –OH to form COOH. It has been found in other studies that an increased fraction of carboxyl group lead higher metal sorption [12].

Column oxidative studies

To understand permanganate reactivity under dynamic conditions a column injection experiment was undertaken. A tracer (KCl) test was carried out before and after MnO_4^- injection. A

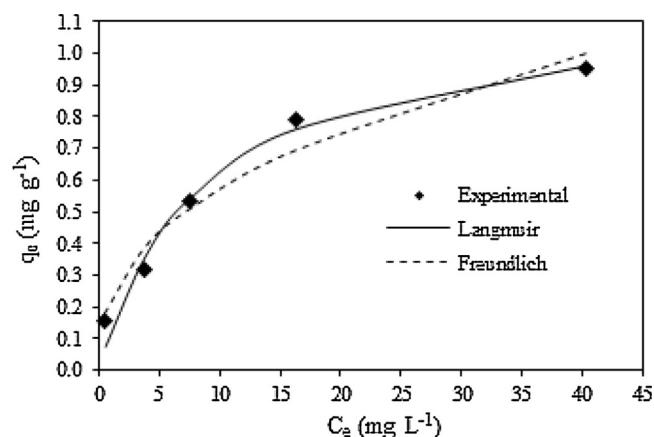


Fig. 7. Prediction of equilibrium sorption model of Zn(II) onto untreated pine.

decrease in porosity (2.3%) was observed between the pre-injection and post MnO_4^- injection tracer test. This suggests that the decrease in porosity due to the precipitation/clogging of MnO_2 on the porous media (pine) was not significant. Breakthrough curves for the permanganate injection are shown in Fig. 5.

The arrival of permanganate was delayed with respect to tracer breakthrough curve which demonstrates that there is a significant reaction between the pine chips and permanganate. The flatter slope of the breakthrough curve for permanganate compared with the tracer is often described as tailing. Tailing is often attributed to physical and/or chemical non-equilibrium between the sorbent and solute. Physical non-equilibrium may result from a diffusional mass transfer. Rate limited diffusion was evident in the intra-particle diffusion plot (Fig. 3). The chemical non-equilibrium from the kinetics of interaction between surface functional groups on the sorbent (pine) and the reactive solute molecule (MnO_4^-) as occur. The batch test showed permanganate reactivity still occurring after 807 min (Fig. 1), however the residence time in the column was only 105 min. Therefore, non-equilibrium reactions were occurring. In total the reaction of pine chips and permanganate was completed after ~ 28 pore volumes (2880 min).

The permanganate consumption estimated from column studies (56 mg g^{-1}) are significantly less than those measured from the batch experiments (436 mg g^{-1}). This may be due to different solid liquid ratios in the batch and column experiments. However, this significant difference needs to be further investigated. Other studies have also observed much lower KMnO_4 consumption (average 0.35 mg g^{-1}) in the column experiments compared to batch experiments ($>1.2\text{ mg g}^{-1}$) using aquifer materials [30].

Batch sorption studies

The sorption kinetics results show that the sorption of Zn(II) was initially rapid followed by a slower process in both the untreated and treated pine chips (Fig. 6).

The sorption kinetics of Zn(II) onto untreated and treated pine chips can be best described by pseudo-second-order due to better

Table 4
Kinetic parameters for the sorption of Zn(II) onto pine.

Pine chips	Pseudo-first-order				Pseudo-second-order			
	k_1 (h^{-1})	q_e (calc) (mg g^{-1})	r^2	SSE	k_2 ($\text{g mg}^{-1}\text{ h}^{-1}$)	q_e (calc) (mg g^{-1})	r^2	SSE
Untreated	0.661	0.71	0.888	0.092	0.858	0.80	0.955	0.060
Treated	0.714	3.4	0.918	0.391	0.228	3.7	0.961	0.286

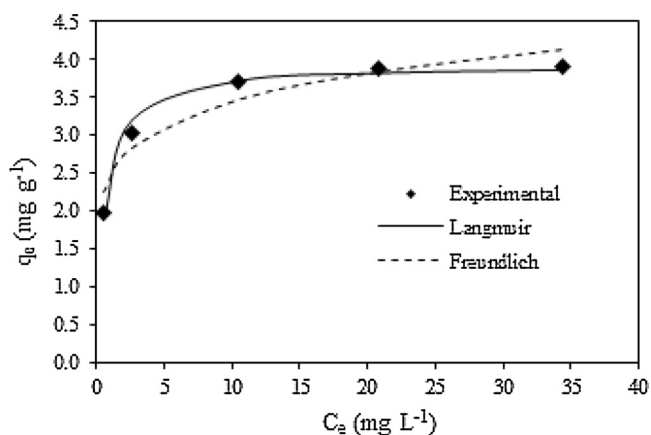


Fig. 8. Prediction of equilibrium sorption model of Zn(II) onto treated pine.

Table 5
Fitted sorption parameters of Zn(II) onto pine.

Pine chips	Langmuir isotherm				Freundlich isotherm			
	Q (mg g ⁻¹)	b (L mg ⁻¹)	r ²	SSE	K	n	r ²	SSE
Untreated	1.2	0.113	0.979	0.042	0.220	0.404	0.959	0.060
Treated	3.9	1.66	0.982	0.098	2.45	0.148	0.918	0.185

goodness of fit parameters (r^2 , SSE) compared to those of the pseudo-first-order kinetic model (Table 4).

This is consistent with the other studies that have successfully applied pseudo-second-order models to many sorption system [24].

Sorption equilibrium experiments were carried out to determine the sorption capacity of untreated and treated pine chips. The equilibrium data were then analysed by Langmuir and Freundlich isotherm equations. The observed data fitted well with the Langmuir model (Figs. 7 and 8 and Table 5). The maximum sorption capacity (Q) of zinc of treated pine chips is higher (3.9 mg g^{-1}) than that the untreated pine chips (1.2 mg g^{-1}).

The initial pH of the batch solution (pH~5) showed a slight decrease with time (0.6 units) for the untreated pine chips and a slight increase for treated pine chips (0.4 units). These pH values are below the value where zinc hydroxide would be expected (i.e. pH > 6) and suggest that zinc removal was mainly due to sorption rather than precipitation.

Conclusions

The research study has provided a solid foundation for understanding the mechanisms involved between permanganate and pine chips. An important outcome from the oxidation of woody biomass (pine) is the increased heavy metal binding capacity. Batch tests showed a significant ~4-fold increase of metal sorption capacity due to chemical modification of the pine chip surface. The permanganate reaction with pine chips comprises a relatively rapid initial reaction and a slower longer term reaction. This was demonstrated in both batch and column studies. This suggests that in-situ modification of pine chips may be viable in treatment barrier systems with a long residence time such as in groundwater barrier systems. It is expected that these outcomes will encourage other researchers and engineers to use modified pine chips as a filtration amendment in biobarrier treatment devices as well as to minimize the landfill space for wood waste. To progress this technology to field application further work on

permanganate-wood reactivity is needed to better understand these reactions under different physico-chemical conditions (e.g. temperature, pH, concentration). Further work is also needed on wastewater-sorbent in-terms of the nature of sorption as well as how using complex synthetic wastewaters with multi-component metal ion solutions with realistic physico-chemical characteristics (e.g. COD, TDS) may impact this.

Acknowledgment

The financial support of this research by the CRC-CARE Pty. Ltd. is gratefully acknowledged.

References

- [1] Environmental Protection Agency (EPA), Toxicological Review of Zinc and Compounds (CAS No. 7440-66-6), EPA/635/R-05/002, Washington, D.C., 2005.
- [2] R. Eisler, Zinc Hazards to Fish, Wildlife, and Invertebrates: A Synoptic Review, US Department of the Interior, Fish and Wildlife Service, Patuxent Wildlife Research Centre, Laurel, MD, 1993.
- [3] S. Rio, P. Martin, Removal of metal ions from aqueous solution by adsorption onto low-cost biosorbent, Environ. Technol. 33 (19–21) (2012) 2211–2215, doi: <http://dx.doi.org/10.1080/09593330.2012.728737>. 23393960.
- [4] A. Kamari, S.N.M. Yusoff, F. Abdullah, W.P. Putra, Biosorption removal of Cu(II), Ni(II) and Pb(II) ions from aqueous solution using coconut dregs residue: adsorption and characterisation studies, J. Environ. Chem. Eng. 2 (4) (2014) 1912–1919, doi: <http://dx.doi.org/10.1016/j.jece.2014.08.014>.
- [5] A.B. Ray, A. Selvakumar, A.N. Tafari, Removal of selected pollutants from aqueous media by hardwood mulch, J. Hazard. Mater. 136 (2) (2006) 213–218, doi: <http://dx.doi.org/10.1016/j.jhazmat.2005.11.094>. 16431019.
- [6] G.S.M. Hossain, R.G. McLaughlan, Sorption of chlorophenols from aqueous solution by granular activated carbon, filter coal, pine and hardwood, Environ. Technol. 33 (16–18) (2012) 1839–1846, doi: <http://dx.doi.org/10.1080/09593330.2011.643554>. 23240177.
- [7] A. Jang, Y. Seo, P.L. Bishop, The removal of heavy metals in urban runoff by sorption on mulch, Environ. Pollut. 133 (1) (2005) 117–127, doi: <http://dx.doi.org/10.1016/j.envpol.2004.05.020>. 15327862.
- [8] A. Demirbas, Heavy metal adsorption onto agro-based waste materials: a review, J. Hazard. Mater. 157 (2–3) (2008) 220–229, doi: <http://dx.doi.org/10.1016/j.jhazmat.2008.01.024>. 18291580.
- [9] D. Sud, G. Mahajan, M.P. Kaur, Agricultural waste material as potential adsorbent for sequestering heavy metal ions from aqueous solutions – a review, Bioresour. Technol. 99 (14) (2008) 6017–6027, doi: <http://dx.doi.org/10.1016/j.biortech.2007.11.064>. 18280151.
- [10] Y. Tsutsumi, A. Islam, C.D. Anderson, K.V. Sarkanen, Acidic permanganate oxidation of lignin and model compounds: comparison with the ozonolysis, Holzforschung 44 (1) (1990) 59–66, doi: <http://dx.doi.org/10.1515/hfsg.1990.44.1.59>.
- [11] K. Garves, Degradation and oxidation of cellulose in acidic potassium permanganate solutions: kinetics and product analyses, Holzforschung 51 (6) (1997) 526–530, doi: <http://dx.doi.org/10.1515/hfsg.1997.51.6.526>.
- [12] G. Jolly, L. Dupont, M. Aplincourt, J. Lambert, Improved Cu and Zn sorption on oxidized wheat lignocellulose, Environ. Chem. Lett. 4 (4) (2006) 219–223, doi: <http://dx.doi.org/10.1007/s10311-006-0051-4>.
- [13] AFIA, Australian Fodder Industry Association Laboratory manual: Acid Detergent Fibre-Wet chemistry—(CSL Method ID: LMOP 2-1108), Acid Detergent Lignin-Wet chemistry; (CSL Lab Manual Operating Procedure 2-1111), Neutral Detergent Fibre-Wet chemistry (CSL Lab Manual Operating Procedure 2-1107), 2010.
- [14] G.E. Rayment, F.R. Higginson, The Australian Laboratory Handbook of Soil and Water Chemical Methods, Inkata Press, Melbourne, 1992.
- [15] N. Seelsaen, R.G. McLaughlan, S. Moore, R.M. Stuetz, Influence of compost characteristics on heavy metals sorption from synthetic stormwater, Water Sci. Technol. 55 (4) (2007) 219–226, doi: <http://dx.doi.org/10.2166/wst.2007.112>. 17425089.
- [16] A.N. Papadopoulos, C.A.S. Hill, A. Gkaraveli, Determination of surface area and pore volume of holocellulose and chemically modified wood flour using the nitrogen adsorption technique, Holz Roh Werkst. 61 (6) (2003) 453–456, doi: <http://dx.doi.org/10.1007/s00107-003-0430-5>.
- [17] Z.S. Wei, Y. Seo, Trichloroethylene (TCE) adsorption using sustainable organic mulch, J. Hazard. Mater. 181 (1–3) (2010) 147–153, doi: <http://dx.doi.org/10.1016/j.jhazmat.2010.04.109>. 20605328.
- [18] G.S.M. Hossain, R.G. McLaughlan, Effect of wood particle size on uptake and desorption study of chlorophenols by woody materials, Environ. Technol. 35 (9–12) (2014) 1484–1490, doi: <http://dx.doi.org/10.1080/09593330.2013.871063>. 24701947.
- [19] C.H. Bolster, G.M. Hornberger, On the use of linearized Langmuir equations, Soil Sci. Soc. Am. J. 71 (6) (2007) 1796–1806, doi: <http://dx.doi.org/10.2136/sssaj2006.0304>.
- [20] E.J. Billo, Excel for Scientists and Engineers: Numerical Methods, Wiley, Hoboken, NJ, 2007.

- [21] S.M.G. Hossain, R.G. McLaughlan, Oxidation of chlorophenols in aqueous solution by excess permanganate, *Water Air Soil Pollut.* 223 (3) (2012) 1429–1435, doi:<http://dx.doi.org/10.1007/s11270-011-0955-x>.
- [22] APHA/AWWA/WEF, Standard Methods for the Examination of Water and Wastewater, 20th ed., American Public Health Association/American Water Works Association/ Water Environment Federation, Washington, D. C, 1998.
- [23] G. Tong, T. Yokoyama, Y. Matsumoto, G. Meshitsuka, Analysis of progress oxidation reaction during oxygen-alkali treatment of lignin I: Method and its application to lignin oxidation, *J. Wood Sci.* 46 (1) (2000) 32–39, doi:<http://dx.doi.org/10.1007/BF00779550>.
- [24] C. Gerente, V.K.C. Lee, P.L. Le Cloirec, G. McKay, Application of chitosan for the removal of metals from wastewaters by adsorption-mechanisms and models review, *Crit. Rev. Environ. Sci. Technol.* 37 (1) (2007) 41–127, doi:<http://dx.doi.org/10.1080/10643380600729089>.
- [25] K.K. Pandey, A study of chemical structure of soft and hardwood and wood polymers by FTIR spectroscopy, *J. Appl. Polym. Sci.* 71 (1999) 1969–1975.
- [26] T.N. Sorrell, *Interpreting Spectra of Organic Molecules*, University Science Books, Mill Valley, CA, 1988.
- [27] M. Kostic, P. Skundric, J. Praskalo, A. Medovic, New functionalities in cellulosic fibers developed by chemical modification, *Hem. Ind.* 61 (2007) 233–237.
- [28] G. Muller, C. Schopper, H. Vos, A. Kharazipour, A. Polle, FTIR-ATR spectroscopic analyses of changes in wood properties during particle and fibreboard production of hard and softwood trees, *Bio. Res.* 4 (2009) 49–71.
- [29] A.M.A. Nada, S. Abd El-Mongy, E.S. Abd el-Sayed, Effect of different treatments on cellulose toward carboxylation and its application for metal ion absorption, *Bio. Res.* 4 (2009) 80–93.
- [30] K.G. Mumford, N.R. Thomson, R.M. Allen-King, Bench-scale investigation of permanganate natural oxidant demand kinetics, *Environ. Sci. Technol.* 39 (8) (2005) 2835–2840, doi:<http://dx.doi.org/10.1021/es049307e>. 15884383.